

Strong spin-lattice coupling and negative thermal expansion in a magnetically frustrated spinel

L. Rossi,^{1,2} A. Bobel,^{1,2} S. Wiedmann,^{1,2} R. K uchler,³
Y. Motome,⁴ K. Penc,⁵ N. Shannon,⁶ H. Ueda,⁷ and B. Bryant^{1,2,*}

¹*High Field Magnet Laboratory (HFML-EMFL), Radboud University, Nijmegen, Netherlands*

²*Radboud University, Institute of Molecules and Materials, Nijmegen, Netherlands*

³*Max Planck Institute for Chemical Physics of Solids, N othnitzer Str. 40, 01187 Dresden, Germany*

⁴*Department of Applied Physics, The University of Tokyo,*

Hongo 7-3-1, Bunkyo-ku, Tokyo 113-8656, Japan

⁵*Institute for Solid State Physics and Optics, Wigner Research Centre for Physics,*

Hungarian Academy of Sciences, Budapest, Hungary

⁶*Okinawa Institute of Science and Technology Graduate University, Japan*

⁷*Department of Chemistry, Graduate School of Science, Kyoto University, Kyoto, Japan*

(Dated: December 17, 2018)

We report on high magnetic field dilatometry measurements of the frustrated spinel CdCr_2O_4 , and discover a distinct negative thermal expansion in the high-field fractional magnetization state. By precisely mapping the phase diagram, and comparing to its counterpart derived from Monte Carlo calculations based on a magnetoelastic theory, we identify a particularly strong spin–lattice coupling in the fractional magnetization state. We show that negative thermal expansion in the pyrochlore lattice can be accounted for within the magnetoelastic theory, as an effect of negative temperature derivative of magnetization and strong spin–lattice coupling.

Frustrated magnets are materials with competing spin interactions, which cannot be simultaneously satisfied. The spin system cannot reach a single magnetic ground state, so it exhibits a huge ground state degeneracy. Spin frustration gives rise to a wide variety of fascinating physical phenomena, such as quantum spin liquids [1] and magnetic monopoles in spin ices [2, 3]. Additionally, frustrated magnets are often found to exhibit negative thermal expansion (NTE), which effect provides a route for the control of thermal expansion necessary to ensure the performance of high–precision devices [4].

In frustrated magnets with a strong coupling between the spin and lattice degrees of freedom, the interplay between magnetic field and spin–lattice coupling produces a range of phases in which frustration is partially relieved. These phases may exhibit NTE, but until now there is no general understanding of the underlying reason for this phenomenon, or how it is linked to spin–lattice coupling.

In this Letter, we report on thermal expansion and magnetostriction measurements of the frustrated spinel CdCr_2O_4 , in magnetic fields up to 30 T. Thermal expansion measurements in high magnetic fields can provide valuable insight into magnetostructural phases: by combining this with the well–known magnetic states, we can explain how strong spin–lattice coupling drives NTE. We map the phase diagram, which we compare to that derived from magnetoelastic theory. The high–field fractional magnetization state exhibits enhanced thermal stability compared to theory, characteristic of a strong spin–lattice coupling in this phase. This state also shows a distinct type of NTE: this effect is accounted for within the framework of the magnetoelastic theory, providing a general result for NTE in pyrochlore lattices.

The pyrochlore lattice, which consists of corner sharing tetrahedra, is a well–known stage for strong geometric frustration [5]. This structure is realized in the position of the Cr^{3+} ions in the chromium spinels ACr_2X_4 , where A is Zn, Cd or Hg and X is O, S or Se. The strength and sign of the Cr–Cr spin coupling depends strongly on the interatomic distance [6, 7], leading to a strong coupling between spin ordering and lattice distortions. The oxide spinels ACr_2O_4 all have antiferromagnetic spin coupling and are magnetically frustrated: because of the frustration they remain paramagnetic down to temperatures well below the Curie–Weiss temperature Θ_{CW} . At T_N the spin frustration is relieved due to a spontaneous lattice distortion [8, 9], which allows a noncollinear spin–spiral antiferromagnetic ground state [10, 11].

The Cr oxide spinels show another magnetostructural transition at high magnetic field, to a fractional magnetization state with one half of the saturation magnetization, in which three of the spins in each tetrahedron are up and one is down [12–16]. This state has a constant magnetization across a wide range of magnetic fields, and it is thus often referred to as the “plateau” state. Both the magnetostructural transition at T_N and the transition to the half–magnetization plateau are manifestations of the strong spin–lattice-coupling in the Cr oxide spinels: a developed magnetoelastic theory [12, 17], describes how the plateau state is stabilized by the spin–lattice coupling.

In order to probe the interplay of frustration and spin–lattice coupling, we performed thermal expansion and magnetostriction measurements of CdCr_2O_4 using capacitive dilatometry at low temperatures and high magnetic fields up to 30 T. This compound was chosen since it is

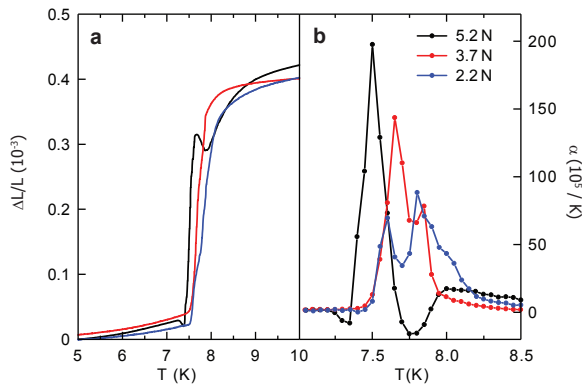


FIG. 1. (color online). Magnetostructural transition at T_N in CdCr_2O_4 , at zero field. (a) Thermal expansion $\Delta L/L$ and (b) thermal expansion coefficient $\alpha = d(\Delta L/L)/dT$ at zero field from 5 K to 10 K with different uniaxial pressure applied. Increasing the force decreases T_N from 7.8 K to 7.5 K.

highly frustrated, with $f = |\Theta_{CW}|/T_N \approx 10$, high quality single crystals are available, and it is possible to reach the plateau phase in static (DC) high field facilities. So far, zero-field thermal expansion measurements [18], and pulsed-field magnetostriction measurements [13], have been reported. We measured the strain $\Delta L/L$ along the [111] direction: the magnetic field is parallel to the [111] direction. The sample is clamped between two plates in the dilatometer, thus applying a small [111] uniaxial pressure. We studied a series of single-crystal samples, all of which are plate-like with wide (111) faces, around 3-5 mm in diameter and between 80 μm and 500 μm thick.

Thermal expansion measurements from 5 K to 10 K at zero field were collected with a capacitive mini-dilatometer in a PPMS [19]. Fig. 1 shows the magnetostructural transition from the cubic $Fd\bar{3}m$, paramagnetic phase to the tetragonal $I4_1/amd$, antiferromagnetic phase on cooling through T_N [18]. Increasing the force applied to the sample from 2.2 N to 5.2 N slightly suppresses T_N from 7.8 K to 7.5 K, and also results in a sharper transition, with a higher thermal expansion coefficient α (Fig. 1(b)). This is an opposite effect to the one seen with the application of hydrostatic pressure, where increasing pressure enhances T_N and Θ_{CW} [7]. We can explain this as due to the applied [111] stress competing with the [001] strain due to the cubic to tetragonal transition. Suppression of antiferromagnetic ordering by uniaxial pressure has also been seen in the chiral magnet MnSi [20].

The data shown in Fig. 1 show a strain of $\approx -4 \times 10^{-4}$ at T_N , slightly larger than the value of -1.6×10^{-4} derived from neutron diffraction data [21] and the similar values reported in previous thermal expansion measurements [18]. This discrepancy can be explained by a slight miscut angle between the [111] axis and the direction of

applied pressure. For high field measurements (Fig. 2) we polished the samples to have parallel and flat surfaces. This helps to reduce the applied pressure in the dilatometer, and so to avoid any ambiguity in the Néel temperature imposed by uniaxial pressure. Polishing had the effect of further increasing the strain observed at T_N , possibly due to an unintended increased miscut or wedge angle between the sample faces.

High field measurements were carried out with the sample mounted in a capacitive dilatometer in a 30 T resistive Bitter magnet [19, 22]. A force similar to the highest force in Fig. 1 was applied. Fig. 2(a) presents thermal expansion from 4.2 K to 10.4 K at zero field and at field increments up to 30 T. The magnetostructural transition at T_N decreases from 7.5 K at zero field to 5.5 K at 27 T, while the measured [111] strain at T_N remains constant. At 26.5 T and at 6.4 K the transition from the high-temperature paramagnetic phase to the low-temperature half-magnetization plateau phase can be seen in the $\Delta L/L$ data as a peak superposed on a step, Fig. 2(b). The appearance or the absence of the peak is sample dependent, while the step was present in all the measured samples. Both phases are cubic - the paramagnetic state $Fd\bar{3}m$, the plateau state $P4_332$ [11] - so from the step we can measure an increase in unit cell volume on cooling, of $\Delta V/V \approx 1.8 \pm 0.9 \times 10^{-4}$. We can explain this increase in volume qualitatively as part of the general principle of the magnetoelastic theory that increased magnetization leads to increased unit cell volume, if antiferromagnetic interactions are assumed [12]. Below this transition and above 27 T, NTE is seen in the plateau phase, shown in Fig. 2(b).

In addition to thermal expansion, constant-temperature magnetostriction measurements were made with field sweeps up to 30 T, at temperatures between 1.3 K and 4.2 K. Fig. 2(c) shows the results from 25 T to 30 T. We see a hysteretic transition from the tetragonal antiferromagnetic phase to the plateau phase, which is consistent with a first order phase transition. Previous pulsed field measurements reported a colossal negative magnetostriction at the transition to the half-magnetization plateau, for both [111] and [110] directions [13, 15]. In our [111] measurements we find a positive magnetostriction at this transition. This is consistent both with measurements on HgCr_2O_4 [23], and with the magnetoelastic theory [12], in which jumps in magnetization are mirrored by unit cell expansion. Both the transition with field to the plateau phase (Fig. 2(c)) and the thermal transition at T_N to the cubic, paramagnetic phase (Fig. 2(a)) have the same sign and similar magnitude in $\Delta L/L$. This indicates that these phases have a similar unit cell, and supports the finding that the plateau phase also has overall cubic symmetry [11, 24].

We also performed a second magnetostriction experiment in a superconductor magnet, between zero and 15 T

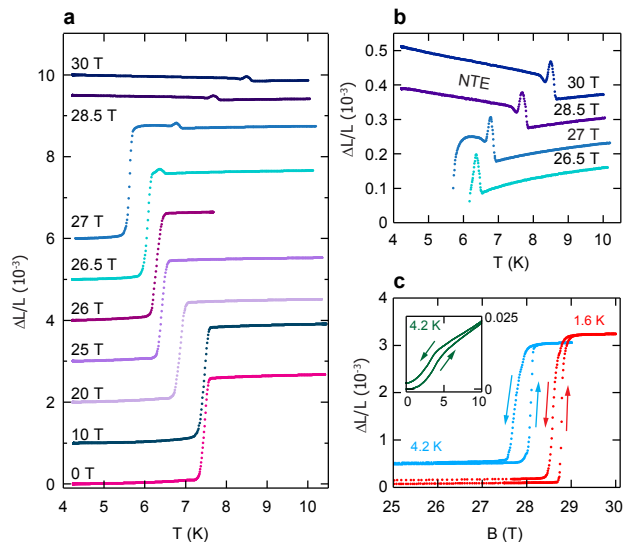


FIG. 2. (color online). Thermal expansion and magnetostriction measurements of CdCr_2O_4 at magnetic fields up to 30 T, used to determine the phase boundaries shown in Fig. 3. (a) Thermal expansion measurements from 4.2 K to 10.4 K in fields up to 30 T, measured on warming, showing the variation of T_N with field. (b) Expansion of data in (a), for fields from 26.5 T to 30 T, showing transition from the paramagnetic state to the half-magnetization plateau state, and the presence of NTE in the plateau state above 27 T. In (a) and (b) the curves have been offset for clarity. (c) Magnetostriction measurements from zero to 30 T at 4.2 K and 1.6 K, showing a hysteretic transition from the antiferromagnetic state to the plateau state. The inset shows magnetostriction up to 10 T at 4.2 K, showing a hysteretic low field transition at around 4.5 T.

and from 2.2 K to 7 K. The inset in Fig. 2(c) presents magnetostriction data at 4.2 K, which show a hysteretic low field transition at around 4.5 T. A similar transition has previously been observed in magnetization data [10, 25]. Based on ESR and optical spectroscopy measurements [25, 26] this has been interpreted as a transition from a helical structure to a commensurate canted spin structure. Neutron diffraction experiments, though, appear to rule out an incommensurate to commensurate transition [10], instead implying a rearrangement of spin spiral domains between 2.5 and 6 T. When the field is in the a - c plane in which the spins rotate in the spiral, a spin-flop is observed: since we apply the field along the [111] direction we would expect a flop to a conical spin spiral.

We can summarize the results from the thermal expansion and magnetostriction measurements in a phase diagram, shown in Fig. 3(a). Three main phases are described: the high-temperature paramagnetic phase, the antiferromagnetic phase below 7.5 K and below 28.7 T, and the high-field half-magnetization plateau phase. Inside the antiferromagnetic phase we identify a low field

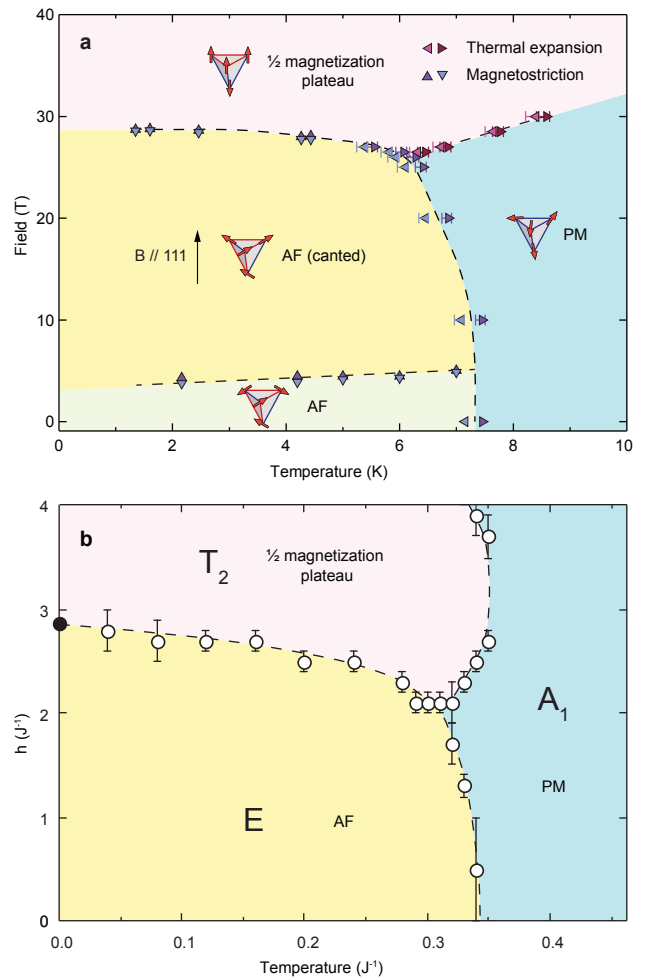


FIG. 3. (color online). Low temperature, high magnetic field phase diagram for CdCr_2O_4 . (a) Experimental phase diagram derived from magnetostriction and thermal expansion measurements, showing the antiferromagnetic (AF) and canted phases, half-magnetization plateau and paramagnetic (PM) phases. Hysteresis is shown by separate points for increasing and decreasing field or temperature. For each phase a schematic spin tetrahedron is shown, with shorter bonds in blue and longer in red. (b) Theoretical phase diagram from Monte Carlo calculations based on the magnetoelastic theory, with the spin-lattice coupling parameter $b = 0.1$: the dominant lattice distortions in each phase (A_1 , E , and T_2) are shown.

transition, which increases from 4.3 T at 2.2 K to 5.1 T at 7 K. Hysteresis is observed in all the transitions. We do not find any experimental evidence of the additional phase transition recently reported from sound velocity measurements [27], though the temperature dependence of the low field transition is consistent with that report. Our new phase diagram is more precise for fields above 12 T than previous diagrams [13, 28].

We can use a magnetoelastic theory to reproduce the experimental phase diagram, and explain the presence of

NTE in the plateau state. A simple, symmetry-driven approach to spin-lattice coupling in Cr spinels, and the corresponding phase transitions in applied magnetic field, was introduced in [12]. In its simplest form, this theory reduces to solving an effective spin model with only two adjustable parameters,

$$\mathcal{H}_{\text{eff}} = J \sum_{\langle ij \rangle} \mathbf{S}_i \cdot \mathbf{S}_j - b (\mathbf{S}_i \cdot \mathbf{S}_j)^2 - h \sum_i S_i^z \quad (1)$$

where $\langle ij \rangle$ are the nearest-neighbor bonds of a pyrochlore lattice, h is the applied magnetic field and J the overall scale of (antiferromagnetic) exchange interactions. $b = J\alpha^2/K$ reflects the strength of the spin-lattice coupling, where K is the elastic constant and α is the spin-lattice coupling. In the case of CdCr_2O_4 , measurements of magnetization lead to an estimate of $b \approx 0.1$ [29].

The effective spin model [Eq. (1)] can be solved using classical Monte Carlo calculations [15, 30], leading to the phase diagram shown in Fig. 3(b). Here, calculations have been carried out for 4-sublattice order, stabilized by an additional third-neighbor interaction $J_3 = -0.05J$ [30]. However, very similar results are obtained for 16-sublattice order [31]. The phase diagram in Fig. 3(b) has been calculated for $b = 0.1$: for purposes of comparison, the results have been scaled for the experimental values of T_N and the critical field H_{c1} .

The Monte Carlo results reproduce the experimental phases well, particularly the B-T dependence of the transitions to the antiferromagnetic phase. The main discrepancy between theory and experimental data is seen in the transition from the paramagnetic phase to the plateau phase, which experimentally has a considerably lower slope in B/T. This indicates that the plateau phase is stable to a higher temperature than the antiferromagnetic phase, as observed experimentally for HgCr_2O_4 [14]. By contrast, the Monte Carlo phase diagram (Fig. 3(b)) predicts that the plateau phase is stable only up to a temperature similar to T_N . In a more general formulation of the magnetoelastic theory, the coefficient of spin-lattice coupling, b , takes on different values in phases in which tetrahedra undergo distortions with different symmetry [12, 32]. In the present case, this leads to three distinct parameters; b_{A_1} (uniform changes in volume); b_E (tetragonal distortions, found in the AF phase); b_{T_2} (trigonal distortions, found in the half-magnetization plateau). From detailed comparison of the magnetoelastic theory to magnetization data for CdCr_2O_4 , Kimura *et al.* [29] obtain $b_{A_1} = 0.05$, $b_E = 0.1$, $b_{T_2} = 0.14$. The Monte Carlo calculations shown in Fig. 3(b) assume $b_{A_1} = b_E = b_{T_2} = 0.1$ so probably underestimate b_{T_2} , and hence the thermal stability of the plateau state, explaining the discrepancy seen between the experimental and theoretical results.

We now turn to the issue of the NTE in the plateau phase. NTE has been seen in several spinel compounds, including CdCr_2S_4 [33] and ZnCr_2Se_4 [34, 35]. CdCr_2O_4 also shows the effect at zero field between 140 K and 45 K [18]. In all these cases the onset of NTE is above the magnetic ordering temperature, and the transition is continuous in $d(\Delta L/L)/dT$. The high field thermal expansion measurements of CdCr_2O_4 here, though, show an abrupt onset of NTE at the transition from the paramagnetic to the half-magnetization plateau phase (Fig. 2(b)). This suggests a mechanism related to the specific properties of the plateau phase.

NTE in pyrochlore lattices is often attributed to strong spin-lattice coupling [18, 33, 34], but a general, microscopic theory is lacking. We can account for the NTE in the plateau phase, via an extension of the previously described symmetry-driven magnetoelastic theory. We find that the dominant magnetic contribution to the thermal expansion comes from the dependence of the A_1 (volume) distortion on the magnetization [36], with the contribution of the E and T_2 distortions being negligible. We can define the magnetic thermal expansion coefficient in terms of the magnetization M and spin-lattice coupling strength α :

$$\frac{\partial}{\partial T} \frac{\Delta L}{L} = \frac{J\alpha}{Kr_0} \frac{8}{3} M \frac{\partial M}{\partial T} + \dots \quad (2)$$

Where r_0 is the equilibrium lattice spacing. We have assumed here that J does not vary with temperature: although in some compounds J is variable [35] we conclude that this is not necessary to produce NTE. NTE will occur when the magnetic contribution to the thermal expansion, given by Eq. (2), is negative and sufficiently large to overcome the normal lattice positive thermal expansion [37]. This condition will be met when the spin-lattice coupling α is large, and the product of M and $\partial M/\partial T$ is large and negative. These conditions are clearly met in the plateau phase of the Cr oxide spinels. The above discussion of the thermal stability of the plateau phase demonstrates a particularly strong spin-lattice coupling, and Monte Carlo calculations, shown in supplementary Fig. S1 and in Ref. [30], show that magnetization is sharply suppressed by increasing temperature in the plateau phase. This is a general result for a spin-only pyrochlore lattice, and we would expect NTE to occur in many pyrochlore compounds where these criteria are met: this is supported by measurements on other Cr spinels. In CdCr_2S_4 , NTE is observed to set in below 98 K in the paramagnetic phase, and persists into the ferromagnetic phase [33]: here $\partial M/\partial T < 0$ in both phases. ZnCr_2Se_4 shows NTE below 75 K, but it is suppressed below $T_N = 21$ K [34, 35], where $\partial M/\partial T > 0$. We would also predict NTE to occur in the high-field saturated magnetization phase of the oxide spinels.

In summary, we made thermal expansion and magnetostriction measurements of the frustrated spinel CdCr_2O_4 , at low temperatures and at magnetic fields up to 30 T. We observe NTE in the plateau phase, which can be explained via a general result from magnetoelastic theory, and the particular properties of this phase, namely strong spin–lattice coupling and negative temperature derivative of magnetization. The experimental phase diagram strongly resembles that produced from Monte Carlo calculations derived from the magnetoelastic theory, but diverges in that the plateau phase is more thermally stable than predicted, providing independent verification of the particularly strong spin–lattice coupling in this phase. The general result provided for the magnetic contribution to thermal expansion in the pyrochlore structure can provide a route to identification of new NTE materials in the future.

This work was supported by the Dutch funding organization NWO-I and by HFML-RU/FOM, a member of the European Magnetic Field Laboratory (EMFL). R.K. is supported by the German Science Foundation through Project No. KU 3287/1-1, and K.P. by Hungarian NK-FIH Grant No. K 124176.

* ben.bryant@ru.nl

- [1] L. Balents, *Nature* **464**, 199 (2010).
- [2] C. Castelnovo, R. Moessner, and S. L. Sondhi, *Nature* **451**, 42 (2008).
- [3] S. T. Bramwell, S. R. Giblin, S. Calder, R. Aldus, D. Prabhakaran, and T. Fennell, *Nature* **461**, 956 (2009).
- [4] K. Takenaka, *Frontiers in Chemistry* **6**, 1 (2018).
- [5] J. S. Gardner, M. J. P. Gingras, and J. E. Greedan, *Reviews of Modern Physics* **82**, 53 (2010).
- [6] A. Yaresko, *Physical Review B* **77**, 115106 (2008).
- [7] H. Ueda and Y. Ueda, *Physical Review B* **77**, 224411 (2008).
- [8] Y. Yamashita and K. Ueda, *Physical Review Letters* **85**, 4960 (2000).
- [9] O. Tchernyshyov, R. Moessner, and S. L. Sondhi, *Physical Review Letters* **88**, 067203 (2002); *Physical Review B* **66**, 064403 (2002).
- [10] M. Matsuda, M. Takeda, M. Nakamura, K. Kakurai, A. Oosawa, E. Lelievre-Berna, J.-H. Chung, H. Ueda, H. Takagi, and S.-H. Lee, *Physical Review B* **75**, 104415 (2007).
- [11] M. Matsuda, K. Ohoyama, S. Yoshii, H. Nojiri, P. Frings, F. Duc, B. Vignolle, G. Rikken, L.-P. Regnault, S.-H. Lee, *et al.*, *Physical Review Letters* **104**, 047201 (2010).
- [12] K. Penc, N. Shannon, and H. Shiba, *Physical Review Letters* **93**, 1 (2004).
- [13] H. Ueda, H. A. Katori, H. Mitamura, T. Goto, and H. Takagi, *Physical Review Letters* **94**, 2 (2005).
- [14] H. Ueda, H. Mitamura, T. Goto, and Y. Ueda, *Physical Review B - Condensed Matter and Materials Physics* **73**, 1 (2006).
- [15] N. Shannon, H. Ueda, Y. Motome, K. Penc, H. Shiba, and H. Takagi, *Journal of Physics: Conference Series* **51**, 31 (2006).
- [16] N. Shannon, K. Penc, and Y. Motome, *Physical Review B* **81**, 184409 (2010).
- [17] D. L. Bergman, R. Shindou, G. A. Fiete, and L. Balents, *Physical Review B - Condensed Matter and Materials Physics* **74**, 1 (2006).
- [18] S. Kitani, M. Tachibana, N. Taira, and H. Kawaji, *Physical Review B* **87**, 064402 (2013).
- [19] R. KÜchler, A. Wörl, P. Gegenwart, M. Berben, B. Bryant, and S. Wiedmann, *Review of Scientific Instruments* **88**, 083903 (2017).
- [20] A. Chacon, A. Bauer, T. Adams, F. Rucker, G. Brandl, R. Georgii, M. Garst, and C. Pfleiderer, *Physical Review Letters* **115**, 1 (2015).
- [21] J.-H. Chung, Y. S. Song, S. Park, H. Ueda, Y. Ueda, and S.-H. Lee, *Journal of the Korean Physical Society* **62**, 1900 (2013).
- [22] R. KÜchler, T. Bauer, M. Brando, and F. Steglich, *Review of Scientific Instruments* **83**, 095102 (2012).
- [23] Y. Tanaka, Y. Narumi, N. Terada, K. Katsumata, H. Ueda, U. Staub, K. Kindo, T. Fukui, T. Yamamoto, R. Kammuri, M. Hagiwara, A. Kikkawa, Y. Ueda, H. Toyokawa, T. Ishikawa, and H. Kitamura, *Journal of the Physical Society of Japan* **76**, 043708 (2007).
- [24] T. Inami, K. Ohwada, M. Tsubota, Y. Murata, Y. H. Matsuda, H. Nojiri, H. Ueda, and Y. Murakami, *Journal of Physics: Conference Series* **51**, 502 (2006).
- [25] S. Kimura, M. Hagiwara, H. Ueda, Y. Narumi, K. Kindo, H. Yashiro, T. Kashiwagi, and H. Takagi, *Physical Review Letters* **97**, 257202 (2006).
- [26] Y. Sawada, S. Kimura, K. Watanabe, and H. Ueda, *Journal of Physics: Conference Series* **568**, 042028 (2014).
- [27] S. Zherlitsyn, V. Tsurkan, A. A. Zvyagin, S. Yasin, S. Erfanifam, R. Beyer, M. Naumann, E. Green, J. Wosnitza, and A. Loidl, *Physical Review B* **91**, 060406 (2015).
- [28] E. Kojima, A. Miyata, S. Miyabe, S. Takeyama, H. Ueda, and Y. Ueda, *Physical Review B* **77**, 212408 (2008).
- [29] S. Kimura, Y. Sawada, Y. Narumi, K. Watanabe, M. Hagiwara, K. Kindo, and H. Ueda, *Physical Review B* **92**, 144410 (2015).
- [30] Y. Motome, K. Penc, and N. Shannon, *Journal of Magnetism and Magnetic Materials* **300**, 57 (2006).
- [31] Y. Motome, K. Penc, and N. Shannon, unpublished (2008).
- [32] K. Penc, N. Shannon, Y. Motome, and H. Shiba, *Journal of Physics: Condensed Matter* **19**, 145267 (2007).
- [33] M. Tachibana, N. Taira, and H. Kawaji, *Solid State Communications* **151**, 1776 (2011).
- [34] J. Hemberger, H.-A. K. von Nidda, V. Tsurkan, and A. Loidl, *Physical Review Letters* **98**, 147203 (2007).
- [35] X. L. Chen, Z. R. Yang, W. Tong, Z. H. Huang, L. Zhang, S. L. Zhang, W. H. Song, L. Pi, Y. P. Sun, M. L. Tian, and Y. H. Zhang, *Journal of Applied Physics* **115**, 083916 (2014).
- [36] See Supplemental Material at [URL].
- [37] G. Hausch, *Physica Status Solidi (a)* **18**, 735 (1973).